J. Phys. B: At. Mol. Opt. Phys. **41** (2008) 025402 (6pp) doi:10.1088/0953-4075/41/2/025402

Robust three-dimensional spatial soliton clusters in strongly nonlocal media

Wei-Ping Zhong[1,2], Lin Yi[1], Rui-Hua Xie[3,4], Milivoj Belić[5] and Goong Chen[6]

[1] State Key Laboratory of Laser Technology, Department of Physics, Huazhong University of Science and Technology, Wuhan 430074, People's Republic of China
[2] Department of Electronic Engineering, Shunde College, Shunde 528300, People's Republic of China
[3] Department of Applied Physics, Xi'an Jiaotong University, Xi'an 710049, People's Republic of China
[4] Department of Mathematics, Texas A&M University, College Station, TX 77843, USA
[5] Texas A&M Univsersity at Qatar, P.O. Box 23874 Doha, Qatar
[6] Department of Mathematics and Institute for Quantum Studies, Texas A&M University, College Station, TX 77843, USA

Received 26 August 2007, in final form 22 November 2007
Published 8 January 2008
Online at stacks.iop.org/JPhysB/41/025402

Abstract
The propagation of three-dimensional soliton clusters in strongly nonlocal nonlinear media is investigated analytically and numerically. A broad class of exact self-similar solutions to the strongly nonlocal Schrödinger equation has been obtained. We find robust soliton cluster solutions, constructed with the help of Whittaker and Hermite–Gaussian functions. We confirm the stability of these solutions by direct numerical simulation. Our results demonstrate that robust higher-order spatial soliton clusters can exist in various forms, such as three-dimensional Gaussian solitons, radially symmetric solitons, multipole solitons and shell solitons.

(Some figures in this article are in colour only in the electronic version)

1. Introduction

Studies of self-similar solutions of nonlinear (NL) differential equations have been of great value in understanding widely different NL physical phenomena [1]. Although self-similar solutions have been extensively studied in many fields such as hydrodynamics and quantum field theory, their applications in optics have not been widespread [2]. Some important results however, have been obtained with previous theoretical studies by considering self-similar behaviour in different systems, for example, in radial pattern formation by counterpropagating beams in transparent cubic-nonlinearity medium [3], NL propagation of pulses with parabolic intensity profiles in optical fibres with normal dispersion [4] and NL compression of chirped Hermite–Gaussian (HG) solitary waves in fibre absorbers [5].

Recent interest in the study of self-trapped optical beams in nonlocal NL media has been stirred by the experimental observation of nonlocal spatial solitons in liquid crystals [6] and lead glasses [7], as well as by some interesting theoretical predictions [8–11]. Some of the predicted properties of nonlocal NL models suggest that in such optical media one should expect stabilization of different types of nonlinear structures, such as necklaces [12] and soliton clusters [13] in two-dimensional (2D) transverse spaces. The creation of 3D solitons, built out of matter waves or NL light in the form of light bullets, presents a great challenge to experiment. One possibility is offered by the Bose–Einstein condensates (BECs) with the attractive interaction between atoms [14]. 3D solitons supported by 3D optical lattices have been reported in [15]. The form of solitons there was predicted by the variational approximation, which was used as an initial guess to generate several examples of stable 3D solitons in direct simulations. Such spatial solitons are essentially confined to one or several cells of the optical lattice. It has also been demonstrated that the localized wave packets in cubic NL materials with a symmetric nonlocal NL response of an arbitrary shape and degree of nonlocality can be described by the general nonlocal nonlinear Schrodinger equation (NNSE). The nonlocality of the nonlinearity prevents beam collapse in optical Kerr media in all physical dimensions, resulting in stable solitary waves under proper conditions

 © 2008 IOP Publishing Ltd Printed in the UK

[10, 11, 16]. Stable 3D spatiotemporal solitons in cubic nonlocal NL media have been reported in [17].

In this paper we study the propagation of light wave packets in strongly nonlocal media, in (3+1)D. We demonstrate the existence of a class of robust soliton waves propagating in a self-similar manner. We find that the predicted self-similar waves can be regarded as clusters of stable 3D spatial solitons.

The paper is organized as follows. In section 2 we introduce a general nonlocal NL model, described by the general NNSE. Section 3 presents the self-similar method of solution of NNSE in the strongly nonlocal limit. Section 4 displays various exact soliton cluster solutions to NNSE. Section 5 brings conclusions.

2. The general nonlocal nonlinear model

We consider evolution of a scalar wave field $u(\mathbf{r}, t)$ governed by the general NNSE in the scaled form:

$$\mathrm{i}\frac{\partial u}{\partial t} + \frac{1}{2}\nabla^2 u + V(\mathbf{r})u + N(I)u = 0, \tag{1}$$

where $V(\mathbf{r})$ is an external potential, $\mathbf{r} = (x, y, z)$ is the scaled 3D position vector and $I = |u|^2$ [10, 11]. The nonlinearity $N(I)$ is assumed of the general nonlocal NL form:

$$N(I) = \int R(r - r')I(r')\,\mathrm{d}^3 r' \tag{2}$$

where the integral is over the whole space and the kernel $R(\mathbf{r})$, also known as the response function, is regular, real, and normalized, $\int R(\mathbf{r})\,\mathrm{d}^3\mathbf{r} = 1$. The nonlinear Schrödinger equation (1) possesses a number of conserved quantities, among them the power $P = \int I(\mathbf{r})\,\mathrm{d}^3\mathbf{r}$, the momentum $\boldsymbol{M} = \int (u^*\nabla u - u\nabla u^*)\,\mathrm{d}^3\mathbf{r}$, the angular momentum $\boldsymbol{L} = \int \mathbf{r} \times (u^*\nabla u - u\nabla u^*)\,\mathrm{d}^3\mathbf{r}$ and the Hamiltonian $H = \int (|\nabla u|^2 + VI - 1/2\,NI)\,\mathrm{d}^3\mathbf{r}$.

The general NNSE model naturally arises in NL optics, where it describes the propagation of an electric field envelope in a wave-guiding potential, in the paraxial approximation. The nonlocal nonlinearity then corresponds to the change in the refractive index of the medium, t corresponds to the propagation distance z and $\mathbf{r} = (x, y)$ spans the 2D transverse space. The nonlocal index change, caused by the propagating beam, involves some transport process in the medium, e.g. heat transfer in materials with thermal nonlinearity [18], diffusion of molecules in atomic vapours [19] or charge separation in photorefractive crystals [20]. The general NNSE also appears in the description of BECs [21, 22], in which case u stands for the collective wavefunction and I is the density of atoms in the condensate. Then V represents the magnetic trap potential, t is the time, and equation (1) becomes the nonlocal Gross–Pitaevskii (GP) equation.

In the limit when the response function $R(\mathbf{r})$ is sharply peaked at a point $\mathbf{r}$ and much narrower than the intensity distribution $I(\mathbf{r})$, the NL term becomes local, $N(I) \approx I$. In NL optics the model (1) then becomes the standard NL Schrödinger equation (SE) with an external potential, describing the local Kerr media. In BECs it becomes the standard GP equation. In the opposite limit, when the response function is much broader than the intensity distribution, the NL term becomes proportional to the response function, $N(I) \approx -PR$, where P is the beam power. Assuming that the intensity distribution is peaked at the origin, one can expand the response function at the origin, to obtain $N(I) \approx -P(R_0 + R_2 r^2)$. In this case the highly *nonlocal nonlinear* SE becomes the *linear* SE with a harmonic potential. A more general treatment in [16], even without the external potential, leads to a NL optical model in which the change in the NL term is proportional to a NL function of the power, $\Delta N(I) \approx -\alpha^2(P)r^2$. Although linear in u, the model still describes a highly NL phenomenon of solitons through the dependence of the coefficient α on the beam power P [16]. For this reason the model is referred to as the *strongly nonlocal* SE. It has been used in [6], for example, to explain the experimental observation of optical spatial solitons in nematic liquid crystals. In this paper we will be concerned with this limit of the general NNSE.

3. Exact self-similar solutions of the strongly nonlocal Schrödinger equation

In the limit of strongly nonlocal nonlinearty, the evolution of an optical field u in three-dimensional media is described by the strongly nonlocal SE [11, 16]:

$$\mathrm{i}\frac{\partial u}{\partial t} + \frac{1}{2}\nabla^2 u - sr^2 u = 0, \tag{3}$$

where t is the evolution coordinate, $\mathbf{r} = (x, y, z)$ spans the 3D 'transverse' coordinate space and s is the parameter proportional to $\alpha^2(P)$, containing the influence of beam power. Note that P is constant, equal to the total input power P_0. Evidently, the same equation describes the time-dependent linear quantum harmonic oscillator. Hence, in solving equation (3) we will also be solving a linear quantum-mechanical problem. Although many different solutions to the *time-independent* quantum harmonic oscillator in different coordinate systems are known, we will be looking for the self-similar *time-dependent* solutions of equation (3) in the form of localized 3D soliton clusters. Such solutions will naturally impose certain conditions on the input parameters and the parameters describing these solutions. It should also be noted that beam collapse cannot occur in equation (3).

The second term in equation (3) represents diffraction and the third term originates from the optical nonlinearity. We treat equation (3) in cylindrical coordinates, by the method of separation of variables. We consider only the case $s > 0$. In cylindrical coordinates, the Laplacian is $\nabla^2 = \frac{1}{\rho}\frac{\partial}{\partial\rho}\left(\rho\frac{\partial}{\partial\rho}\right) + \frac{1}{\rho^2}\frac{\partial^2}{\partial\varphi^2} + \frac{\partial^2}{\partial z^2}$, where φ is the azimuthal angle, $r^2 = \rho^2 + z^2$ and $\rho^2 = x^2 + y^2$. The separation of variables $u(t, z, \rho, \varphi) = U(t, \rho)\Phi(\varphi)G(t, z)$ in equation (3) leads to the following three equations:

$$\frac{\mathrm{d}^2\Phi}{\mathrm{d}\varphi^2} + m^2\Phi = 0, \tag{4a}$$

$$\mathrm{i}\frac{\partial U}{\partial t} + \frac{1}{2\rho}\frac{\partial}{\partial\rho}\left(\rho\frac{\partial U}{\partial\rho}\right) - \frac{m^2}{2\rho^2}U - s\rho^2 U - \mu U = 0, \tag{4b}$$

$$\mathrm{i}\frac{\partial G}{\partial t} + \frac{1}{2}\frac{\partial^2 G}{\partial z^2} - sz^2 G + \mu G = 0, \tag{4c}$$

where μ and m are non-negative real constants. From equation (4a) we have $\Phi_m(\varphi) = \cos(m\varphi) + \mathrm{i}q\sin(m\varphi)$, where the parameter q ($0 \leqslant q \leqslant 1$) determines the modulation depth of the beam intensity [23].

Now we solve equation (4b) using the self-similar method. Following [24], we define the complex field as $U(t,\rho) = A_1(t,\rho)\exp[\mathrm{i}B_1(t,\rho)]$, where A_1 and B_1 are the real functions of t and ρ. Substituting $U(t,\rho)$ into equation (4b), we find the following two coupled equations for the phase $B_1(t,\rho)$ and the amplitude $A_1(t,\rho)$:

$$-\frac{\partial B_1}{\partial t} + \frac{1}{2}\left[\frac{1}{A_1}\frac{\partial^2 A_1}{\partial \rho^2} - \left(\frac{\partial B_1}{\partial \rho}\right)^2 + \frac{1}{\rho A_1}\frac{\partial A_1}{\partial \rho}\right] - \frac{m^2}{2\rho^2} - \mu - s\rho^2 = 0, \tag{5a}$$

$$\frac{1}{A_1}\frac{\partial A_1}{\partial t} + \frac{1}{2}\left(\frac{2}{A_1}\frac{\partial B_1}{\partial \rho}\frac{\partial A_1}{\partial \rho} + \frac{\partial^2 B_1}{\partial \rho^2} + \frac{1}{\rho}\frac{\partial B_1}{\partial \rho}\right) = 0. \tag{5b}$$

To find a self-similar solution of equation (4b), we assume that the amplitude and the phase have the form [24] $A_1(t,\rho) = \frac{k_1 P_0}{w_1(t)} F(\theta_1)$ and $B_1(t,\rho) = a_1(t) + b_1(t)\rho + c_1(t)\rho^2$, respectively. Here k_1 is the normalization constant and P_0 is the initial power of the beam. Other variables are defined as follows: $w_1(t)$ is the beam width, $F(\theta_1)$ is a real function to be determined, $\theta_1(t,\rho)$ is the self-similar variable and $a_1(t)$ is the phase offset. The functions $\theta_1(t,\rho)$, $b_1(t)$ and $c_1(t)$, defined by the form of A_l and B_l, are found from equation (5b): $\theta_1(t,\rho) = \frac{\rho^2}{w_1^2}$, $b_1(t) = 0$ and $c_1(t) = \frac{1}{2w_1}\frac{\mathrm{d}w_1}{\mathrm{d}t}$. The amplitude $A_1(t,\rho)$ is found from equation (5a) by solving the following differential equation:

$$-\frac{w_1^2}{2}\left(\frac{\mathrm{d}a_1}{\mathrm{d}t} + \mu\right)F + \frac{\mathrm{d}F}{\mathrm{d}\theta_1} + \theta_1\left[\frac{\mathrm{d}^2 F}{\mathrm{d}\theta_1^2} + \frac{w_1^2}{2}\left(-\frac{w_1}{2}\frac{\mathrm{d}^2 w_1}{\mathrm{d}t^2} - s w_1^2\right)F\right] - \frac{m^2 F}{4\theta_1} = 0. \tag{6}$$

Inserting a variable transformation $F(\theta_1) = \theta_1^{-\frac{1}{2}} f(\theta_1)$, after some algebra we arrive at

$$\frac{\mathrm{d}^2 f}{\mathrm{d}\theta_1^2} + \left[\frac{w_1^2}{2}\left(-\frac{w_1}{2}\frac{\mathrm{d}^2 w_1}{\mathrm{d}t^2} - s w_1^2\right) - \frac{1}{\theta_1}\frac{w_1^2}{2}\left(\frac{\mathrm{d}a_1}{\mathrm{d}t} + \mu\right) + \frac{1}{\theta_1^2}\frac{1-m^2}{4}\right] f = 0. \tag{7}$$

Setting

$$\frac{w_1^2}{2}\left(-\frac{w_1}{2}\frac{\mathrm{d}^2 w_1}{\mathrm{d}t^2} - s w_1^2\right) = -\frac{1}{4}, \tag{8a}$$

$$-\frac{w_1^2}{2}\left(\frac{\mathrm{d}a_1}{\mathrm{d}t} + \mu\right) = n, \tag{8b}$$

one gets the following equation from equation (7):

$$\frac{\mathrm{d}^2 f}{\mathrm{d}\theta_1^2} + \left[-\frac{1}{4} + \frac{n}{\theta_1} + \frac{\frac{1}{4} - \left(\frac{m}{2}\right)^2}{\theta_1^2}\right] f = 0, \tag{9}$$

where n is a real number. Equation (9) is the well-known Whittaker differential equation, whose solutions are known as the Whittaker functions [25]:

$$f(\theta_1) = \Psi_{nm}(\theta_1) = \frac{\mathrm{e}^{-\frac{\theta_1}{2}}\theta_1^n}{\Gamma\left(\frac{1}{2} - n + 2m\right)} \times \int_0^\infty \tau^{-n-\frac{1}{2}+2m}\left(1 + \frac{\tau}{\theta_1}\right)^{n-\frac{1}{2}+2m}\mathrm{e}^{-\tau}\,\mathrm{d}\tau, \tag{10}$$

where the real part is $\mathrm{Re}[n - 1/2 - 2m] \leqslant 0$, and $n - 1/2 - 2m$ is not an integer. Γ is the Gamma function. Equation (8*a*) is re-expressed as

$$\frac{1}{2}\left(\frac{\mathrm{d}\eta}{\mathrm{d}t}\right)^2 + \frac{2s w_0^4(\eta^2 - 1)(\eta^2 - \lambda)}{\eta^2} = 0, \tag{11}$$

where $\eta = w_1/w_0$ and $\lambda = 1/2s w_0^4$. Here the subscript '0' denotes the initial value of the corresponding quantity at $z = 0$. Taking $\eta(t)|_{t=0} = 1$ and $\mathrm{d}\eta(t)/\mathrm{d}t|_{t=0} = 0$, and integrating equation (11) yields

$$w_1^2 = w_0^2\left[\cos^2\left(2\sqrt{s}w_0^2 t\right) + \lambda\sin^2\left(2\sqrt{s}w_0^2 t\right)\right]. \tag{12}$$

Hence, when $\lambda = 1$ the beam diffraction is exactly balanced by the nonlocality. Since $w_1 = w_0$ for $\lambda = 1$, the beam width is not connected with the propagation distance. Rather, the wave packet size becomes independent of time. It is clearly seen that the beam becomes an accessible soliton [16]. The parameters can now be determined, and they are given by $w_1 = w_0$, $c_1 = 0$ and $a_1(t) = a_{10} - \mu t - \frac{2nt}{w_0^2}$. Thus, the exact self-similar soliton solution of equation (4b) can be written as

$$U_{nm}^{\mathrm{sol}}(t,\rho,\varphi) = \frac{k_1 P_0}{\rho}\psi_{nm}\left(\frac{\rho^2}{w_0^2}\right)\mathrm{e}^{\mathrm{i}a_1(t)}. \tag{13}$$

Next, we seek the solution of equation (4c) using the same method. We obtain the self-similar solution of equation (4c) in the form of HG functions [2]:

$$G(t,z) = A_2(t,z)\,\mathrm{e}^{\mathrm{i}B_2(t,z)}, \tag{14a}$$

$$A_2(t,z) = \frac{k_2}{\sqrt{w_2(t)}}\exp\left(\frac{1}{2} - \frac{\theta_2^2}{2}\right)H_l(\theta_2), \tag{14b}$$

$$B_2(t,z) = a_2(t) + b_2(t)z + c_2(t)w_2^2\theta_2^2, \tag{14c}$$

where $k_2 = \left(\frac{1}{2^l l!\sqrt{\pi}}\right)^{1/2}$ and l is a non-negative integer. $H_l(\theta_2)$ are Hermite polynomials of the lth order, and θ_2 and b_2 are given by $\theta_2(t,z) = \frac{z}{w_2}$, $b_2 = 0$. The remaining parameters $w_2(t)$, $a_2(t)$ and $c_2(t)$ take the form

$$w_2^2 = w_0^2\left[\cos^2\left(2\sqrt{s}w_0^2 t\right) + \lambda\sin^2\left(2\sqrt{s}w_0^2 t\right)\right], \tag{15}$$

$$\frac{\mathrm{d}a_2}{\mathrm{d}t} = -\mu - \frac{2l+1}{w_2^2}, \tag{16}$$

$$c_2(t) = \frac{1}{2w_2}\frac{\mathrm{d}w_2}{\mathrm{d}t}. \tag{17}$$

When $\lambda = 1$ this solution also becomes an accessible soliton. The above parameters are then given by $w = w_0$, $a_2 = a_{20} - \mu - \frac{(2n+1)t}{w_0^2}$, $c_2 = 0$. Hence, we obtain the HG self–similar soliton solution to equation (4c):

$$G_l^{\mathrm{sol}}(t,z) = \frac{k_2\exp[\mathrm{i}a_2]}{\sqrt{w_0}}\,\mathrm{e}^{\frac{1}{2}-\frac{z^2}{2w_0^2}}H_l\left(\frac{z}{w_0}\right). \tag{18}$$

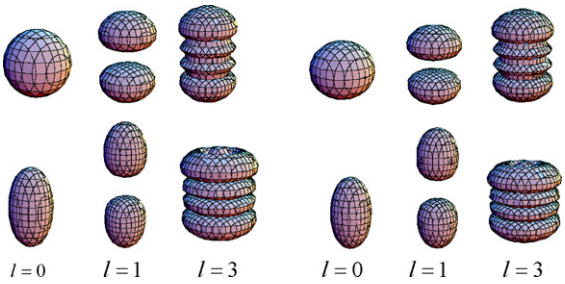

Figure 1. Comparison of the analytical solution for intensity with the numerical simulation, for different n and l, when $m = 0$. Here the parameter l is taken to have the values $l = 0, 1, 3$ from left to right. (a) Analytical solution of equation (19) for $n = 0$ (top) and $n = 1$ (bottom). (b) Numerical simulation of equation (3) for $n = 0$ (top) and $n = 1$ (bottom).

Putting all the partial solutions together, we finally obtain the exact self-similar soliton solution of equation (3):

$$u_{lnm}^{\mathrm{sol}}(t, z, r, \varphi) = \frac{kP_0}{\rho\sqrt{w_0}}[\cos(m\varphi) + \mathrm{i}q\sin(m\varphi)] \times H_l\left(\frac{z}{w_0}\right)\psi_{nm}\left(\frac{\rho^2}{w_0^2}\right)\mathrm{e}^{\frac{1}{2}-\frac{z^2}{2w_0^2}+\mathrm{i}a(t)}, \tag{19}$$

where $k = k_1k_2$, $a = a_1 + a_2$ and $\rho^2 = x^2 + y^2$.

4. The form of the 3D spatial soliton clusters

We note that the novel 3D spatial solitons in equation (19) are determined by the three parameters *l, n,* and *m*. These 3D spatial solitons form clusters having some common characteristics. We will present contour plots of the optical field distributions in 3D for some specific values of the parameters, choosing the initial conditions to be $w_0 = 1$ and $P_0 = 1$.

4.1. The general 3D spatial soliton clusters (m is a non-negative integer)

4.1.1. Gaussian soliton clusters ($m = 0$). When $m = 0$ one obtains the Gaussian soliton clusters. In figure 1 a comparison of the analytical solution with the numerical simulation with different n and l for the Gaussian soliton clusters is presented. Numerical solution of equation (3) is performed to ascertain the stability of soliton clusters and to compare with the analytical solution. As expected, no collapse is seen [11], and excellent agreement with the analytical solution is obtained. Strikingly, there are l-layer ellipsoids along the vertical (z-axis) direction. The larger the n, the longer the ellipsoid's major axis length. The maximum optical intensity is located at the outside layer ellipsoids, along the vertical direction. Obviously, when all of the three parameters are zero, the soliton forms a sphere which is called the fundamental Gaussian soliton in the 3D space.

4.1.2. Radially symmetric soliton clusters ($q = 1$, $m > 0$). For $m > 0$, in the limit $q = 1$ there exist radially symmetric soliton clusters. In figure 2 we show some properties of the radial soliton clusters. It is seen that for the same m, the larger the parameter n, the thicker the cluster along the vertical direction. The optical intensity is zero at the central point $(x, y, z) = (0, 0, 0)$. The soliton distribution does not depend on the azimuthal angle.

As seen in figures 1 and 2, the Gaussian soliton clusters and the radially symmetric soliton clusters display a well-defined symmetry. The physical origin of the phenomenon can qualitatively be understood from the nature of nonlocality. Nonlinear nonlocality here means that the NL polarization of the medium has the symmetry of the electric field. Owing to the additional assumption of strong nonlocality, resulting in a harmonic potential, the distributions of the optical field and the intensity are obviously independent of the azimuthal angle.

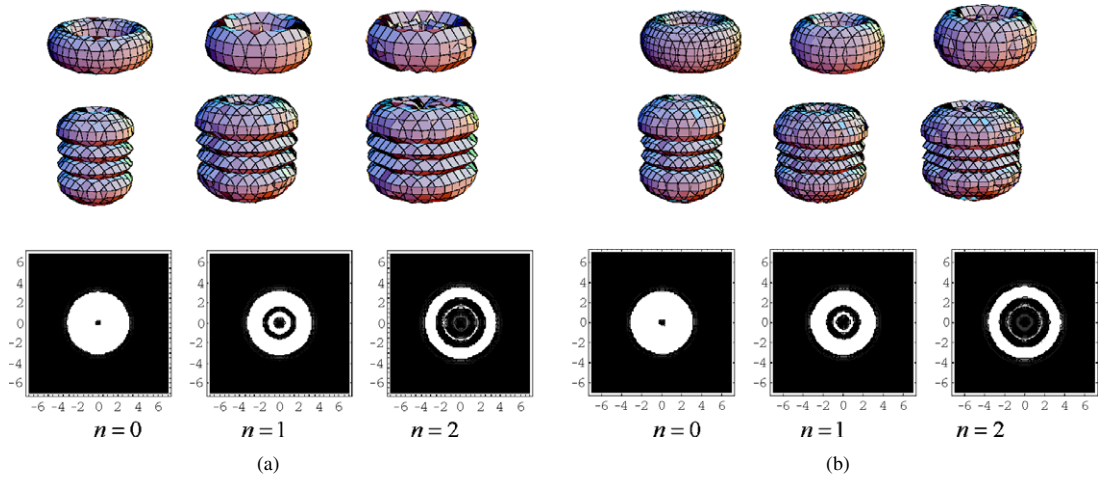

Figure 2. Intensity distributions of the radially symmetric soliton clusters when $q = 1$, $m = 1$. Here the parameter n is taken to have values $n = 0, 1, 2$ from left to right. (a) Analytical solution of equation (19) for $l = 0$ (top) and $l = 3$ (middle). (b) Numerical simulation of equation (3) for $l = 0$ (top) and $l = 3$ (middle). The bottom row presents the vertical view from directly above.

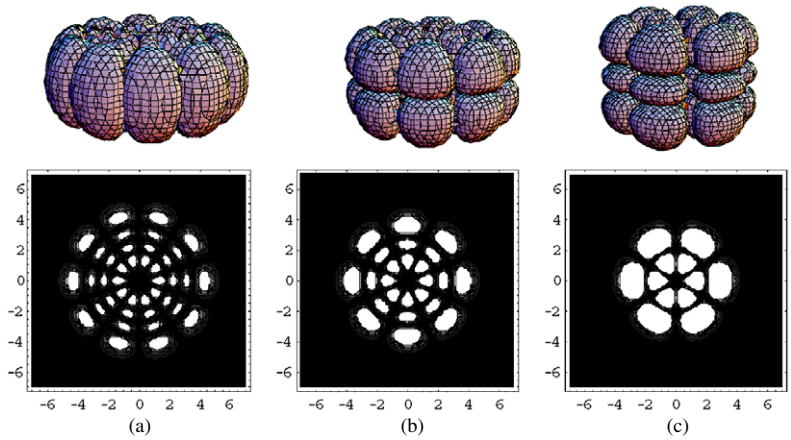

Figure 3. Top row: soliton cluster intensity distributions with different parameters. Bottom row represents the vertical view from directly above. The parameters are taken as follows: (a) $n = 3, l = 0, m = 5$; (b) $n = 2, l = 1, m = 4$; (c) $n = 1, l = 2, m = 3$ from left to right, respectively.

4.1.3. Multipole soliton clusters ($q = 0$, $m \neq 0$). In the limit $q = 0$ and for $m \neq 0$, we observe multipole soliton clusters with different parameters (n, m, l). These multipole solitons contain single-layer necklace soliton clusters ($n = 0$, $m \neq 0$) and multi-layer necklace soliton clusters (n positive integer, $m \neq 0$). In figure 3 we present some examples of the multipole soliton clusters.

Interesting structures are seen for the multipole soliton clusters in 3D. We find that the larger the parameter m, the larger the necklace radius. It is seen that the distributions change regularly with the azimuthal angle. When m is large enough, the ellipsoids form a necklace soliton ring. The number of ellipsoids in each layer is decided by m, and the layer number is decided by n, in the horizontal direction. These multipole soliton clusters have $2m(n + 1)(l + 1)$ ellipsoids, and form $n + 1$ necklace layers in the horizontal plane and $l + 1$ layers in the vertical direction.

These characteristics can be explained easily. In a strongly nonlocal NL medium, the refractive index is determined by the intensity distribution over the entire transverse coordinate space, and under proper conditions the nonlocality can lead to an increase of the refractive index in the overlap region, giving rise to the formation of multipole solitons. Note that when the nonlocal response function is much wider than the beam itself, the range of nonlocality in the medium is very large and the width of the refractive index distribution greatly exceeds the width of an individual light spot.

4.2. Shell soliton clusters (0 < m < 1, a non-negative fraction)

For $q = 0$, $0 < m < 1$ a non-negative fraction, and l equal to n, we show in figure 4 some examples of optical field intensity distributions, which we call 'shell soliton clusters'. They display an internally layered structure. As seen, the larger the parameter n, the larger the cylinder length along the vertical direction. When $m \to 0$ they form an ellipsoid.

For $q = 1$, $m > 0$ (m is a fraction less than one) and l identical with different integers n, we show in figure 5 the optical field intensity distribution for $m = \frac{1}{2}$ and different n. They form the shell soliton clusters, consisting of multiple

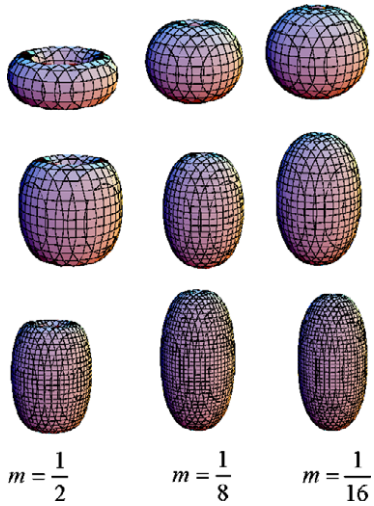

Figure 4. Comparison of optical field intensity distributions for $q = 0, l = 0$, with different m $(0 < m < 1)$ and integer n. Here the parameter n is equal to 0, 1, 3 from top to bottom.

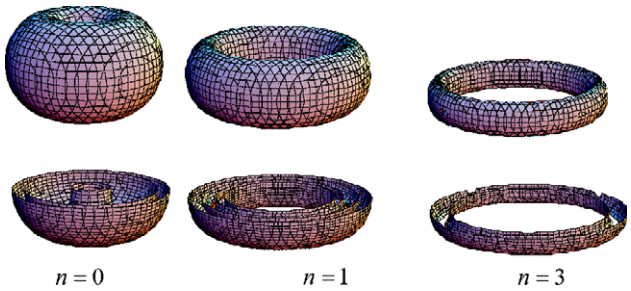

Figure 5. Optical field intensity showing four, three and two layers when $q = 1, l = 0$, $m = \frac{1}{2}$ and different n. Bottom row is a cross-section through $z = 0$, which clearly displays the shell structure.

layers. As seen, the larger the parameter n, the thinner the cylinder thickness along the vertical direction and the greater the radius of the internal ring. The optical field consists of four layers, three layers and two layers, respectively, depending on $n = 0, 1, 3$.

5. Conclusion

We have studied 3D self-similar spatial soliton clusters in strongly nonlocal media, both analytically and numerically. An analytical solution has been obtained, and numerical simulation has been performed, to confirm the stability of solutions. We found that robust 3D spatial soliton clusters exist, even though the starting strongly nonlocal SE is linear. It should be pointed out that the nonlinear polarization of media has the symmetry of the electric field, due to strong nonlocality. The distribution of the optical field is then independent of the azimuthal angle. Under proper conditions, the nonlocality leads to a change of the refractive index in the overlap region, giving rise to the formation of three-dimensional Gaussian solitons, radially symmetric solitons, multipole solitons, and shell solitons.

Acknowledgments

This work was supported by the National Science Foundation of China under grant No. 2006CB921605 and the Science Research Foundation of Shunde College, China.

References

[1] Barenblat G I 1996 *Scaling, Self-Similarity, and Intermediate Asymptotics* (Cambridge: Cambridge University Press)
[2] Chen S, Yi L, Guo D and Lu P 2005 *Phys. Rev.* E **72** 016622
[3] Afanas'ev A A, Kruglov A, Samson B A, Jakyte R and Volkov V M 1991 *J. Mod. Opt.* **38** 1189
[4] Chen S and Yi L 2005 *Phys. Rev.* E **71** 016606
[5] Chen S, Liu H, Zhang S and Yi L 2006 *Phys. Lett.* A **353** 493
[6] Conti C, Peccianti M and Assanto G 2004 *Phys. Rev. Lett.* **92** 113902
[7] Rotschild C, Cohen O, Manela O, Segev M and Carmon T 2005 *Phys. Rev. Lett.* **95** 213904
[8] Krolikowski W and Bang O 2000 *Phys. Rev.* E **63** 016610
[9] Krolikowski W, Bang O, Rasmussen J J and Wyller J 2001 *Phys. Rev.* E **64** 016612
[10] Wyller J, Krolikowski W, Bang O and Rasmussen J J 2002 *Phys. Rev.* E **66** 066615
[11] Bang O, Krolikowski W, Wyller J and Rasmussen J J 2002 *Phys. Rev.* E **66** 046619
[12] Soljacic M and Segev M 2001 *Phys. Rev. Lett.* **86** 420
[13] Desyatnikov A S and Kivshar Yu S 2002 *Phys. Rev. Lett.* **88** 053901
[14] Malomed B A, Mihalache D, Wise F and Torner L 2005 *J. Opt. B: Quantum Semiclass. Opt.* **7** R53
[15] Baizakov B B, Malomed B A and Salerno M 2003 *Europhys. Lett.* **63** 642
[16] Snyder A W and Mitchell D J 1997 *Science* **276** 1538
[17] Mihalache D, Mazilu D, Lederer F, Malomed B A, Kartashov Y V, Crasovan L C and Torner L 2006 *Phys. Rev.* E **73** 025601(R)
[18] Kartashov Y V, Vysloukh V A and Torner L 2007 *Opt. Express* **15** 9378
[19] Skupin S, Saffman M and Krolikowski W 2007 *Phys. Rev. Lett.* **98** 263902
[20] Krolikowski W, Saffman M, Luther-Davies B and Denz C 1998 *Phys. Rev. Lett.* **80** 3240
[21] Dalfovo F, Giorgini S, Pitaevskii L P and Stringari S 1999 *Rev. Mod. Phys.* **71** 463
[22] Perez-Garcia V M, Konotop V V and Garcia-Ripoll J J 2000 *Phys. Rev.* E **62** 4300
[23] Lopez-Aguago S, Desyatnikov A S, Kivshar Y S, Skupin S, Krolikowski W and Bang O 2006 *Opt. Lett.* **31** 1100
[24] Zhong W P and Yi L 2007 *Phys. Rev. A* **75** 061801(R)
[25] Whittaker E T and Watson G N 1990 *A Course in Modern Analysis* 4th edn (Cambridge: Cambridge University Press)